

On the seasonal variation of air – sea CO₂ fluxes in the outer Changjiang (Yangtze River) Estuary, East China Sea

Weidong Zhai, Minhan Dai *

State Key Laboratory of Marine Environmental Science, Xiamen University, Xiamen 361005, China

ARTICLE INFO

Article history:

Received 1 November 2008

Received in revised form 23 February 2009

Accepted 24 February 2009

Available online 9 March 2009

Keywords:

Carbon dioxide

Air – sea flux

Changjiang Estuary

East China Sea

ABSTRACT

Based upon seven field surveys conducted during April 2005 – April 2008, we examined the surface partial pressure of CO₂ (*p*CO₂) and dissolved oxygen (DO) in the outer Changjiang (Yangtze River) Estuary, on the inner shelf of the East China Sea (ECS). This area represents a most dynamic zone of the ECS where high *p*CO₂ riverine water meets with highly productive shelf waters, covering a 2° × 3° area, ~10% of the surface area of the entire ECS. Surface *p*CO₂ ranged 320 – 380 μatm (average ~345 μatm) in winter, 180 – 450 μatm (average ~330 μatm) in spring, 150 – 620 μatm (average ~310 μatm) in summer and 120 – 540 μatm (average ~375 μatm) in autumn. The seasonal variation pattern of surface DO generally mirrored that of *p*CO₂, ranging 95% – 105% in winter, 96% – 142% (average 110%) in spring, 73% – 192% (average 118%) in summer and 81% – 178% (average 102%) in autumn. The dynamics of *p*CO₂ drawdown and DO enhancement in the warm seasons (from April to October) appeared to be controlled by primary productivity and air – sea exchange, while mixing dominated the aqueous *p*CO₂ in the cold seasons (from November to March of the following year). This study showed that the outer Changjiang Estuary served as a moderate or significant sink of atmospheric CO₂ in winter, spring and summer, while it turned to a net source in autumn. The integrated sea – air CO₂ flux in the outer Changjiang Estuary was estimated as $-1.9 \pm 1.3 \text{ mol m}^{-2} \text{ year}^{-1}$, which is double the recent sea–air CO₂ flux estimation for the northern ECS.

© 2009 Elsevier B.V. All rights reserved.

1. Introduction

Coastal waters, despite comprising only a small portion of the world's ocean surface area, play a critically important role in the global oceanic carbon cycle and have recently received increasing attention (e.g. Cai and Dai, 2004; Borges et al., 2005; Muller-Karger et al., 2005; Cai et al., 2006; Chen and Borges, 2009). Determination of the variability of surface CO₂ partial pressure (*p*CO₂) and hence the air – sea CO₂ flux remains a huge challenge primarily due to the dynamic nature of the coastal waters. More difficulty is added in the nearshore systems such as the inner shelf region, which result in even more complexity. Generally, these systems receive large upwelled and riverine inputs of both carbon and nutrients, fueling both high biological production and respiration (Chen and Borges, 2009), as a result of which physical and biogeochemical processes interplay and greatly affect the carbon dynamics.

The East China Sea (ECS) is one of the world's major marginal seas. Together with the Yellow Sea to its north, this interconnected continental shelf system is the world's broadest continental shelf and one

of the most productive areas in the world's oceans (Gong et al., 1996, 2003; Wong et al., 2000). This is at least partially due to the nutrient supply from one of the world's largest rivers, the Changjiang (Yangtze River). The ECS is also well documented as a typical shelf system located at mid-latitude and referred to as a sink of atmospheric CO₂ (Zhang et al., 1997; Tsunogai et al., 1999; Wang et al., 2000; Hu and Yang, 2001; Shim et al., 2007). It must be pointed out that direct *p*CO₂ measurements in the ECS are very limited and the reported air – sea CO₂ fluxes have been mostly in the open area of the ECS. In the most heterogeneous inner shelf region, however, only a few sporadic data have been reported (e.g. Tan et al., 2004; Zhai et al., 2007; Chen et al., 2008), which clearly hampers our ability to accurately estimate the overall air – sea CO₂ flux of the ECS.

A better understanding of the ECS CO₂ flux is fundamental before it can be placed in a global context. In this study, we looked at seven direct *p*CO₂ and dissolved oxygen (DO) measurement surveys in the outer Changjiang Estuary during 2005 – 2008, together with another two data sets collected in August 2003 (Chen et al., 2008) and January 2006 (Zhai et al., 2007) in the same area of the Changjiang Estuary. These data sets provide us *p*CO₂ with higher resolution than before both in time and space to examine the seasonality of the air – sea CO₂ fluxes of the outer Changjiang Estuary. This region, covering a 2° × 3° area, represents ~10% of the total ECS surface area (Fig. 1), and is a highly dynamic zone both in terms of physical and biogeochemical processes (see below).

* Corresponding author. Environmental Science Research Center, Xiamen University, 422 Si-ming Nan-lu, Xiamen, 361005, China. Tel.: +86 592 2182132; fax: +86 592 2180655.

E-mail address: mdai@xmu.edu.cn (M. Dai).

2. Materials and methods

2.1. Study area

Both the ECS and the Changjiang Estuary are in a temperate climatic region with a cold/dry winter (from December to early March of the following year) and a warm/wet summer (from June to early September). In the western ECS, the water column is well mixed in winter. According to Tsunogai et al. (1999), besides the biological productivity that enhances CO₂ uptake, the formation of denser water resulting from the intensive winter cooling nearshore may help to transport much CO₂ to the deeper open ocean via isopycnal mixing and advection. Such a combined physical and biological process introducing atmospheric CO₂ into the ocean has been referred to as a “continental shelf pump” (Tsunogai et al., 1999). Note that in summer, the water column is stratified owing to surface heating and the freshwater input (Li et al., 2002; Shim et al., 2007; Zhang et al., 2007).

The focal area of this study is located in the inner shelf of the ECS, off the Changjiang Estuary mouth (i.e. the outer Changjiang Estuary, Fig. 1), where high pCO₂ waters discharged from the river meets with highly productive ECS waters (Zhai et al., 2007; Chen et al., 2008). Induced primarily by the high rates of nutrient supply from the Changjiang River, algal blooms and significant surface pCO₂ drawdown frequently occur in this region in flooding months, during May – August (Chen et al., 2003; Tan et al., 2004). Hypoxia (bottom DO < 60 μmol O₂ kg⁻¹) has also been reported in the poorly ventilated bottom waters in the outer Changjiang Estuary (Li et al., 2002; Wei et al., 2007; Chen et al., 2007; Zhang et al., 2007). This hypoxia appears in June (Chen et al., 2007; Zhang et al., 2007) and peaks in August – September with an area of > 12,000 km² (Li et al., 2002; Wei et al., 2007), while it tends to disappear after October as a result of strong vertical mixing (Zhang et al., 2007). This large and

highly heterogeneous regime may have a significant impact on the overall CO₂ budget of the ECS.

Fig. 1 summarizes all those published researches related to air – sea CO₂ fluxes in the ECS and the Changjiang Estuary. Tsunogai et al. (1997, 1999) report a net air – sea CO₂ flux of $-2.9 \text{ mol m}^{-2} \text{ year}^{-1}$ extrapolated from the relationship of pCO₂ and other parameters obtained from 14 stations along the PN line (from 31.4°N 123.0°E through to 27.5°N 128.4°E) (Fig. 1). Wang et al. (2000) survey the carbonate system in spring and summer in the east part of the ECS and calculate the pCO₂. These authors further compile pCO₂ data in autumn and winter from Tsunogai et al. (1997) and estimate a net air – sea CO₂ flux of -1.2 to $-2.8 \text{ mol m}^{-2} \text{ year}^{-1}$. However, Shim et al. (2007) obtain a relatively smaller net air – sea CO₂ flux of $-0.87 \text{ mol m}^{-2} \text{ year}^{-1}$, based on four sampling cruises (1 in spring, 1 in summer and 2 in autumn) of pCO₂ underway measurements and use the Wanninkhof (1992) empirical function of wind speed. According to Zhang et al. (1997), Zhang et al. (1999) and Hu and Yang (2001), the air – sea CO₂ flux is only -0.2 to $-0.9 \text{ mol m}^{-2} \text{ year}^{-1}$ based on four surveys covering a seasonal cycle and ~50 stations interspersed along three crossing-shelf transects and the east side transect in the ECS.

Our previous studies have shown that the inner Changjiang Estuary is a moderate CO₂ source to the atmosphere (Zhai et al., 2007) with elevated surface pCO₂. The relatively high pCO₂ values (>600 μatm) near the estuary mouth are clearly extended off the estuary mouth, as seen in both winter and summer from the present study (Fig. 2). However in the focal region under study, this typical high-pCO₂ riverine water was located in a very limited area (Fig. 2).

2.2. Sampling and analyses

During April 2005 – April 2008, seven cruises were carried out onboard R/Vs Kexue 3 and Dongfanghong II in the outer Changjiang Estuary (Fig. 2; Table 1). Sea surface temperature (SST), salinity, pCO₂ and DO were measured using our underway pumping system (modified from Zhai et al., 2005, 2007) and more recently using an automated flowing pCO₂ measuring system (GO8050, General Oceanics Inc., USA). In the September – October 2006 cruise, discrete water samples for Winkler DO were also obtained at five or six depths with 8-L Niskin bottles mounted with a CTD unit (SBE-17-plus, Sea Bird Co.).

During these surveys, a Li-Cor® non-dispersive infrared (NDIR) spectrometer (Li-7000) was used to measure CO₂ molecular fractions (xCO₂) in the equilibrator and in the air (Zhai et al., 2005, 2007; Chen et al., 2008). For the purpose of air – sea flux estimation, the atmospheric pCO₂ was corrected to 100% humidity at *in situ* SST and salinity. For calibration purposes, a series of CO₂ gas standards with xCO₂ values from 200 to 1000 μmol mol⁻¹ were applied. The uncertainty of these standards was ~1%, which represents the maximum level of uncertainty during the period of extensive measuring of pCO₂ and data processing (see details in Zhai et al., 2005, 2007) prior to November 2006. Since our November 2006 cruise, we have been able to reduce this uncertainty to ~0.3% based on two calibration experiments (November 2006 and December 2007) with L.X. Zhou's laboratory, the Centre for Atmosphere Watch And Services (CAWAS) in the Chinese Academy of Meteorological Sciences, whose CO₂ standard reference gases were directly from CCGG/ESRL/NOAA (uncertainty <0.03%). However, if we include the uncertainty caused by the residue water vapor in the line before the NDIR detector of the GO8050 system, typically 0.5–1.6 mmol H₂O mol⁻¹ during standard gas checks and 4–5 mmol H₂O mol⁻¹ for atmospheric CO₂ measurements and ~2 mmol H₂O mol⁻¹ for aqueous CO₂ measurements, the additional uncertainty due to the H₂O signal is estimated as ~0.5% (<2 μatm for a pCO₂ value at the atmospheric level). Therefore, the overall uncertainty during the pCO₂ measuring and data processing is still ~1% in this study. This was further confirmed during the November 2007 cruise by a synchronous comparison experiment between the GO8050 system and our previously used underway pumping system (modified from Zhai et al., 2005, 2007).

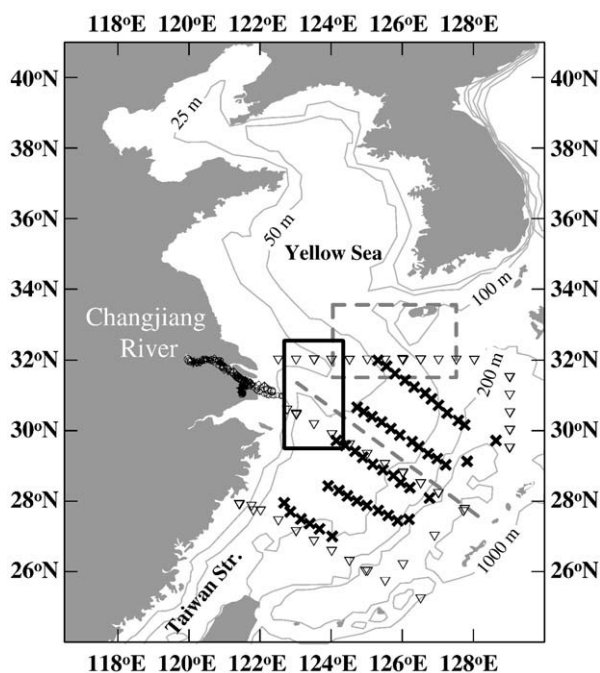


Fig. 1. Area map and a summary of published studies that have estimated air – sea CO₂ fluxes in the East China Sea and neighboring regions. The rectangular area (122°20' – 124°20'E, 29°30' – 32°30'N) represents the focal area in this study, while the dashed rectangular area in the northern East China Sea has been studied by Shim et al. (2007). The grey dashed line from 31.4°N 123.0°E through to 27.5°N 128.4°E is the PN line reported in Tsunogai et al. (1997, 1999). “x” symbols show the stations sampled by Wang et al. (2000), while downward facing triangles show sampling stations of Zhang et al. (1997, 2001). Air – water CO₂ fluxes in the neighboring inner estuary of the Changjiang River have been reported by Zhai et al. (2007). The Yellow Sea to the north, Changjiang to the west, Taiwan Strait to the South and isobaths of 25-, 50-, 100-, 200- and 1000-m are also shown.

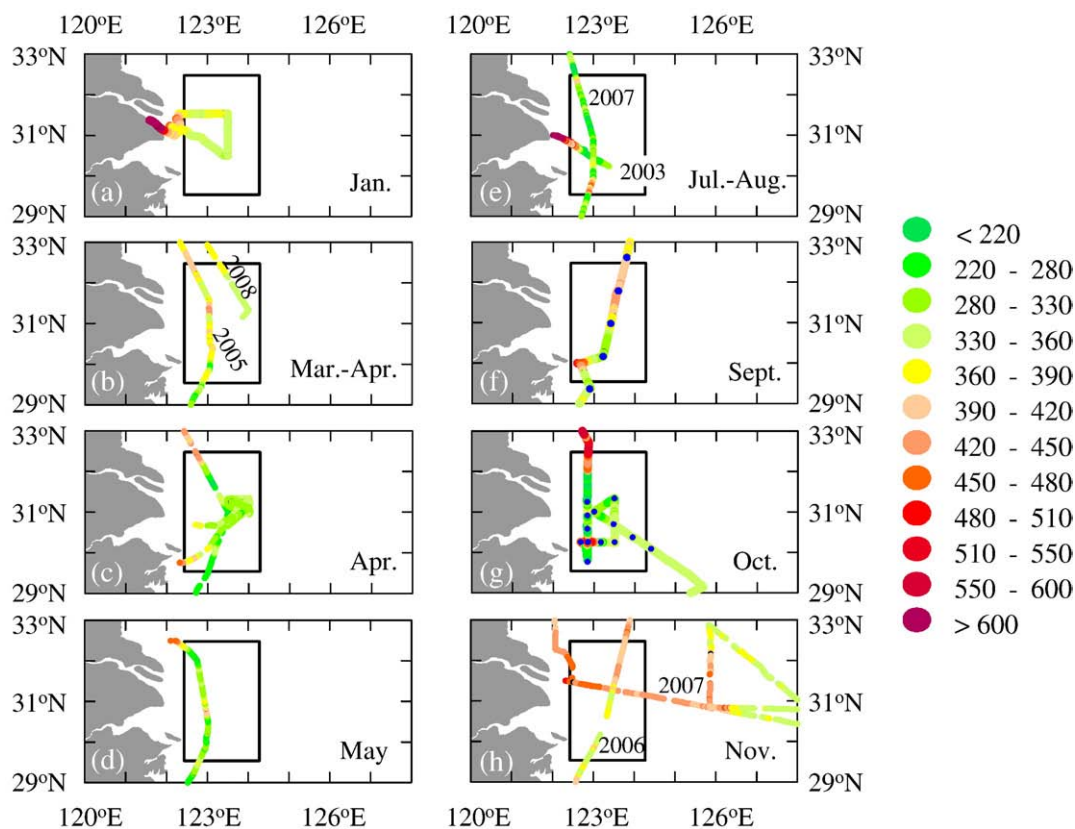


Fig. 2. Seasonal aqueous $p\text{CO}_2$ distribution (in μatm) during the underway pumping surveys, including January 2006 for winter (a); late March 2008 and early April 2005 (b); April 2008 (c) and May 2005 (d) for spring; August 2003 and July 2007 for summer (e); September–October 2006 (f, g); November 2006 and November 2007 (h) for autumn. Yellow color represents the atmospheric $p\text{CO}_2$ level of 360–390 μatm , while warm or cold colors show aqueous $p\text{CO}_2$ higher or lower than the atmospheric $p\text{CO}_2$ level. The rectangular area refers to Fig. 1, i.e. the air–sea CO_2 flux estimation area in this study. Discrete samples were collected at water depths in September–October 2006 in sampling sites shown in panels (f) and (g).

Ancillary data such as salinity, temperature, DO and fluorometric Chl-a were continuously measured with a YSI® 6600 meter and/or a WTW's Cellox® 325 probe (see details in Zhai et al., 2005, 2007). Recently we used a set of Idronaut Multiparameter “Flow Through” sensor modules to support the salinity, temperature and DO data from the G08050 system. Discrete samples for Winkler DO were also collected for post-calibration purposes (Zhai et al., 2007). To estimate air–sea transfer velocities of CO_2 , a set of meteorological sensors (R.M. Young Company, USA) was used to measure the 10-m wind speed.

2.3. Sea–air CO_2 flux estimation

Average net CO_2 fluxes (F) were estimated based on the formula $F = k \times K_H \times \Delta p\text{CO}_2$, where k is the gas transfer velocity of CO_2 , K_H is the solubility of CO_2 (Weiss, 1974), and $\Delta p\text{CO}_2$ is the mean difference between the water and air $p\text{CO}_2$. A positive flux value represents the net CO_2 exchange from the water body to the atmosphere and a negative

value refers to the net exchange from the atmosphere to the water body. Since the on site k value is not available, our calculations have been based on the Wanninkhof (1992) empirical function of wind speed:

$$k(\text{cm h}^{-1}) = 0.31 \times u^2 \times (\text{Sc}/660)^{-0.5}$$

where k is the gas transfer velocity; u is the field-measured wind speed in m s^{-1} at 10-m height, here recorded by our onboard meteorological sensors; Sc is the Schmidt number of CO_2 in seawater; 660 is the Sc value in seawater at 20 °C.

3. Results

3.1. Hydrological settings

Water discharge of the Changjiang River is subject to significant seasonal variation (Zhai et al., 2007). Overall, our January cruise

Table 1
Sampling cruise summary.

Surveying time	Season	Sampling type (pumping intake depth)	Underway CO_2 system configuration	Ref.
August 25–27, 2003	Summer	Surface underway pumping (1.5 m)	Modified from Zhai et al. (2005, 2007)	Chen et al. (2008)
April 06–09, 2005	Spring	Surface underway pumping (5 m)	Modified from Zhai et al. (2005, 2007)	This study
May 13–16, 2005	Spring	Surface underway pumping (5 m)	Modified from Zhai et al. (2005, 2007)	This study
January 01–03, 2006	Winter	Surface underway pumping (1.5 m)	Modified from Zhai et al. (2005, 2007)	Zhai et al. (2007)
September 18–October 17, 2006	Autumn	Surface underway pumping (3 m) + Water column station (Niskin bottles)	Modified from Zhai et al. (2005, 2007)	This study
November 20–24, 2006	Autumn	Surface underway pumping (5 m)	Modified from Zhai et al. (2005, 2007)	This study
July 01–06, 2007	Summer	Surface underway pumping (5 m)	Modified from Zhai et al. (2005, 2007)	This study
November 01–10, 2007	Autumn	Surface underway pumping (5 m)	G08050	This study
March 28–April 30, 2008	Spring	Surface underway pumping (5 m)	G08050	This study

represented the cold/dry winter; the cruises from March to May showed the spring; our July/August cruises reflected the typical summer and flood season; and the other cruises from September to November denoted the autumn (Table 1). The salinity change was much reflective of such a seasonal pattern, and decreased from 32.7 ± 1.2 in winter through 27–33 in spring to the lowest 28 ± 4 in summer (Table 2). In autumn, salinity returned to a relatively high value of 29–34 (Table 2). SST changed from lower values of 12.5 ± 1.7 °C in winter and 10–18 °C in spring to high values in summer (26.2 ± 3.0 °C) and in autumn (19–26 °C) (Table 2).

3.2. Distributions of sea surface $p\text{CO}_2$ and other biogeochemical properties

In our spring and summer surveys, most $p\text{CO}_2$ fell in the range between 220 and 350 μatm in the outer Changjiang Estuary (Figs. 2b–e, 3a). Note that in one of our spring cruises in early April 2005, $p\text{CO}_2$ was frequently measured as ~ 400 μatm , slightly higher than the atmospheric $p\text{CO}_2$ level (Figs. 2b, 3a). In winter, aqueous $p\text{CO}_2$ ranged between 321 and 377 μatm , overall lower than the atmospheric $p\text{CO}_2$ level (Fig. 2a; Table 2). In contrast, we observed a $p\text{CO}_2$ level generally higher than the atmosphere in autumn in the northern part of the outer Changjiang Estuary (Fig. 3b), especially in late autumn in November (Fig. 2h). In the southern part of the outer Changjiang Estuary, most aqueous $p\text{CO}_2$ levels ranged between 300 and 370 μatm in September and November 2007, substantially higher than the above-mentioned $p\text{CO}_2$ range in spring and summer (Fig. 3a, b). An exception occurred in our October 2006 survey, when a significant $p\text{CO}_2$ drawdown (down to 120–250 μatm) was evident in the outer Changjiang Estuary (Figs. 2g; 3b). This low $p\text{CO}_2$ area appeared to be extended beyond the study area into the west part of the ECS (Fig. 2g). It is also worth noting that the November 2007 data set had a larger spatial coverage, which showed relatively high $p\text{CO}_2$ in the west part of the ECS

and lower $p\text{CO}_2$ in the east part in autumn, a pattern which is similar to that reported by Shim et al. (2007).

Our data therefore have clearly shown significant spatial variability of aqueous $p\text{CO}_2$ as well as possible intra-seasonal variations. Such intra-seasonal variability can also be seen from other water properties (e.g. chlorophyll fluorescence shown in Fig. 3c) in spring (April and May) of 2005 and autumn (September, October and November) of 2006. It should be pointed out that these “intra-seasonal” variations in autumn were revealed in different years and thus whether inter-annual changes are given significant weight deserves further study. Nevertheless, in the study area a generally high $p\text{CO}_2$ in the autumn as compared to the other three seasons was evident from this study (Figs. 2, 3a–b).

The seasonal cycle of sea surface $p\text{CO}_2$ and other water properties are further summarized in Fig. 4. Accompanied with the lowest salinity and highest SST (Fig. 4a–b), the summer $p\text{CO}_2$ was overall lowest (320 ± 110 μatm , Fig. 4c). Tan et al. (2004) also report that sea surface $p\text{CO}_2$ values were down to as low as 117 μatm in July–August 2001 in approximately the same area. In winter and spring, aqueous $p\text{CO}_2$ was 347 ± 14 μatm and 336 ± 74 μatm , respectively. In contrast to the above three seasons, most aqueous $p\text{CO}_2$ in our two November cruises (382 ± 29 μatm in 2006 and 450 ± 21 μatm in 2007, Table 2) were higher than the atmospheric $p\text{CO}_2$ (370–390 μatm during the two cruises).

Generally, the seasonal variation of DO mirrored the $p\text{CO}_2$ (Fig. 4c, d). DO saturation was generally highest in summer and lowest in autumn. In winter, surface DO ranged 95%–104% (Table 2; Zhai et al., 2007), very close to an equilibrium level with the air. In summer, the highest DO saturation was $\sim 190\%$ in August 2003 (Chen et al., 2008) and $> 160\%$ in July 2007 (Table 2). In spring, a highly oversaturated DO of $\sim 140\%$ was observed in April 2005 and April 2008 (Table 2). In autumn, DO was mostly close to the air-equilibrium level (Fig. 4d), although highly oversaturated DO was also observed in September and October 2006 (Table 2). However, in early November 2007, DO was overall

Table 2

Water temperature, salinity, DO saturation and $p\text{CO}_2$ (mean \pm S.D.) in the outer Changjiang Estuary under study.

Surveying dates	SST (°C)	Surface salinity	DO (%)	Aqueous $p\text{CO}_2$ (μatm)	Air $p\text{CO}_2$ (μatm)
August 25 – 27, 2003	28.2 ± 1.0 (26.0 – 29.7)	26.4 ± 2.6 (17.4 – 31.4)	124 ± 27 (81 – 192)	318 ± 106 (181 – 621)	363 ± 3 (359 – 366)
April 06 – 09, 2005	11.1 ± 0.8 (8.6 – 12.2)	28.9 ± 1.6 (24.3 – 32.0)	107 ± 8 (100 – 140)	373 ± 37 (222 – 453)	383 ± 4 (378 – 390)
May 13 – 16, 2005	16.8 ± 1.0 (15.5 – 19.4)	29.6 ± 1.4 (26.3 – 31.6)	107 ± 5 (96 – 118)	308 ± 45 (214 – 454)	375 ± 2 (372 – 379)
January 01 – 03, 2006	12.5 ± 1.7 (8.0 – 15.3)	32.7 ± 1.2 (28.1 – 34.2)	~ 100 (94 – 105)	347 ± 14 (321 – 377)	384 ± 4 (380 – 391)
September 20, 2006	25.0 ± 0.5 (23.9 – 25.9)	33.0 ± 1.1 (28.6 – 33.9)	101 ± 7 (91 – 138)	384 ± 56 (293 – 515)	362 ± 2 (361 – 366)
October 15 – 17, 2006	24.7 ± 0.8 (23.3 – 26.3)	31.7 ± 2.7 (22.1 – 33.8)	110 ± 15 (89 – 178)	326 ± 78 (121 – 538)	371 ± 3 (367 – 377)
November 20 – 24, 2006	21.0 ± 0.9 (19.8 – 22.6)	33.3 ± 0.3 (32.2 – 33.6)	100 ± 3 (95 – 105)	382 ± 29 (343 – 448)	378 ± 3 (373 – 382)
July 01 – 06, 2007	24.2 ± 0.9 (21.8 – 26.0)	29.8 ± 2.0 (21.9 – 32.3)	111 ± 17 (73 – 165)	304 ± 68 (154 – 479)	378 ± 5 (370 – 388)
November 01 – 10, 2007	21.2 ± 1.0 (19.1 – 22.2)	32.8 ± 1.4 (29.9 – 34.0)	92 ± 7 (81 – 102)	450 ± 21 (418 – 488)	386 ± 2 (384 – 390)
March 30, 2008	10.4 ± 0.6 (9.7 – 11.6)	33.1 ± 0.6 (32.3 – 34.1)	111 ± 1 (110 – 114)	353 ± 10 (332 – 365)	390 ± 2 (389 – 392)
April 01 – 08, 2008 ^a	12.1 ± 0.6 (10.8 – 13.3)	34.1 ± 0.4 (33.1 – 34.6)	112 ± 3 (108 – 121)	322 ± 11 (300 – 347)	390 ± 4 (383 – 398)
April 08 – 10, 2008	12.5 ± 0.2 (12.0 – 13.0)	32.6 ± 1.2 (29.3 – 34.5)	109 ± 2 (102 – 121)	314 ± 21 (258 – 374)	389 ± 5 (382 – 395)
April 11 – 18, 2008 ^a	12.8 ± 0.4 (11.7 – 13.6)	34.1 ± 0.2 (33.5 – 34.4)	110 ± 3 (105 – 130)	319 ± 10 (263 – 337)	391 ± 3 (385 – 397)
April 18 – 19, 2008	13.5 ± 0.4 (12.5 – 14.7)	32.8 ± 1.3 (29.1 – 34.2)	118 ± 10 (105 – 135)	301 ± 37 (247 – 400)	390 ± 1 (389 – 391)
April 28 – 29, 2008	15.2 ± 1.2 (12.9 – 18.3)	30.1 ± 2.2 (25.1 – 33.4)	120 ± 8 (109 – 147)	298 ± 67 (181 – 443)	387 ± 1 (386 – 388)

Field data in August 2003 and January 2006 are from Chen et al. (2008) and Zhai et al. (2007) respectively.

^a This survey was conducted in a limited area, covering $123^{\circ}29'$ – $124^{\circ}00'$ E, $31^{\circ}00'$ – $31^{\circ}21'$ N.

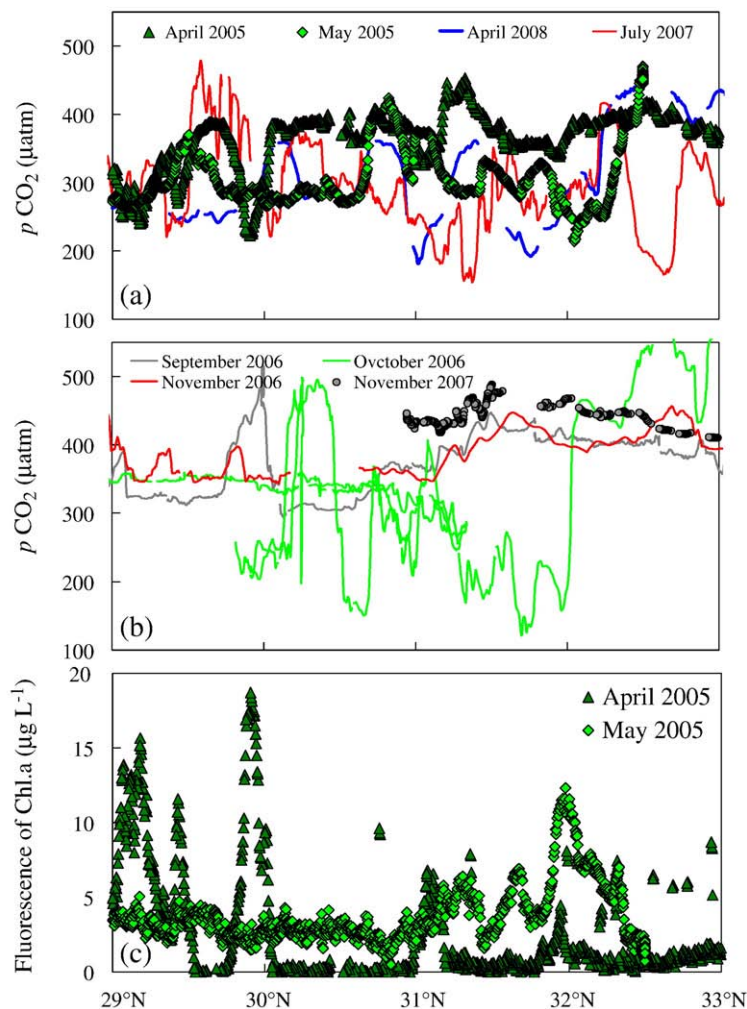


Fig. 3. Spatial variations of $p\text{CO}_2$ in spring/summer (a) and autumn (b) in the outer Changjiang Estuary. Also shown is the comparison of surface fluorescence of Chl-a between the two spring surveys (along the same transect) in 2005 (c).

undersaturated in the outer Changjiang Estuary (Table 2), which was the only time this was seen in this study.

4. Discussion

4.1. Factors influencing sea surface $p\text{CO}_2$

SST and salinity have effects on aqueous $p\text{CO}_2$ (Fig. 5). In warm seasons (from April to October), the relationship of SST vs. $p\text{CO}_2$ was generally random (Fig. 5a), while water mixing may have affected the $p\text{CO}_2$ dynamics to some extent in the low salinity zone at $S < 27$ (Fig. 5b). However, for salinity at $S \sim 27 - 32$, the overall random relationship between $p\text{CO}_2$ and salinity (Fig. 5b) revealed a major effect of non-physical (i.e. metabolic) processes on $p\text{CO}_2$ dynamics. In cold seasons (from November to March of the following year), $p\text{CO}_2$ and SST were apparently correlated with each other (Fig. 5c). The similarly negative correlations between $p\text{CO}_2$ and salinity in Fig. 5d suggest that the aqueous $p\text{CO}_2$ in the cold seasons was mainly dominated by mixing between the low-temperature / high- $p\text{CO}_2$ estuarine or coastal water and the high-temperature / low- $p\text{CO}_2$ ECS water.

This difference in different seasons (mixing modulated $p\text{CO}_2$ distribution in cold seasons and coupled controls by physical mixing and non-physical processes) is apparently associated with the primary production levels. According to Gong et al. (2003), significantly enhanced primary production is only observed in summer. In the cold seasons of the year (e.g., in winter and in early spring), primary

production remains low, at about 10% of the summer value due to low temperature and low light availability (Gong et al., 2003).

In order to further examine the above-mentioned non-physical processes influencing the CO_2 dynamics in warm seasons, we plotted $p\text{CO}_2$ vs. DO saturation (Fig. 6). The arrows in Fig. 6a illustrate possible physical and biogeochemical forcings on the relationship between $p\text{CO}_2$ and DO. Heating / cooling had significant effects on both the $p\text{CO}_2$ and DO% ($4.23\% \text{ } ^\circ\text{C}^{-1}$ vs. $1.60\% \text{ } ^\circ\text{C}^{-1}$) in the same direction, while primary production / aerobic respiration also affected both $p\text{CO}_2$ and DO according to the Redfield stoichiometry at a given chemical buffering capacity level (see the caption of Fig. 6 for details). On the other hand, air – sea exchange had a bigger impact on DO than $p\text{CO}_2$ because the air – sea re-equilibration of $p\text{CO}_2$ is approximately 90% slower than DO due to the chemical buffering capacity of the marine carbonate system.

The $p\text{CO}_2$ – DO relationship in April 2005 and the summers of 2003/2007 overall followed the predicted Redfield line (Fig. 6), which suggested that both the DO enhancement and $p\text{CO}_2$ drawdown during these surveys were modulated by in situ metabolic processes (primary production and respiration). The significant coupling between DO and Chl-a (not shown) provided additional evidence for these metabolically dominant $p\text{CO}_2$ – DO dynamics. In May 2005 however, the slope of the $p\text{CO}_2$ – DO plot significantly departed from the typical Redfield line (Fig. 6b). It furthermore greatly departed from the slope of the $p\text{CO}_2$ – DO plot derived from April 2005 (-8.6 vs. -4.2 , Fig. 6b), although the two surveys were conducted along the

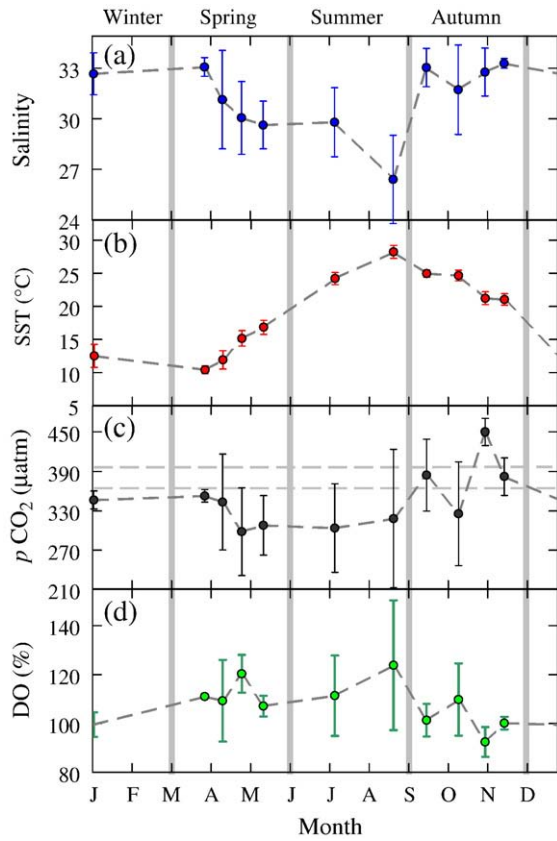


Fig. 4. Seasonal cycles of salinity, SST, $p\text{CO}_2$ and DO saturation in the outer Changjiang Estuary. Two horizontal dash lines in panel (c) show the atmospheric CO_2 level (Table 2).

same transect with an interval of only 1 month (Fig. 2b–c; Table 1). It is thus suggested that the on-site metabolic processes in April and the month long air – sea exchange since April (see arrows in Fig. 6b for reference) may have resulted in the unique pattern of the $p\text{CO}_2$ – DO relationship in May 2005. The relatively homogeneous but lower Chl-a

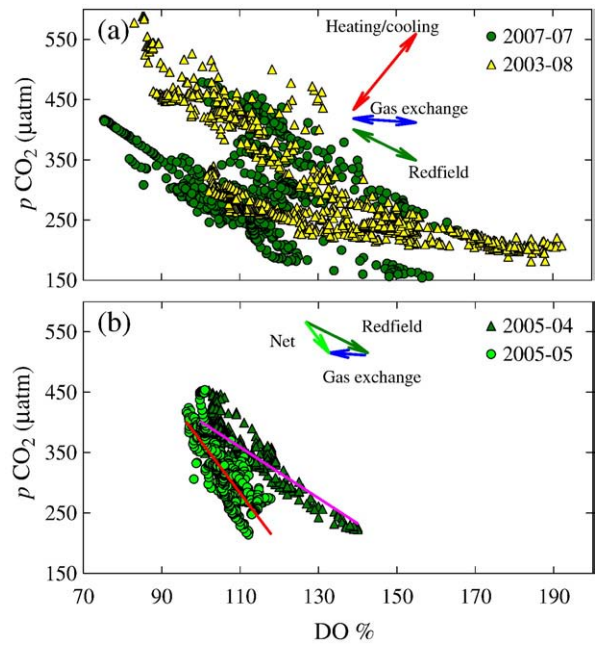


Fig. 6. Relationships between $p\text{CO}_2$ and DO saturation during our summer surveys (a) and the two 2005 spring surveys (b) in the outer Changjiang Estuary. The arrows illustrate possible physical and biogeochemical forcings. The solid lines in panel (b) are regression lines, fitted by minimizing the sum of the squares of the y-offsets, $y = -4.2x + 822.0$ ($R^2 = 0.70$) for the April 2005 survey and $y = -8.6x + 1228.5$ ($R^2 = 0.65$) for the May 2005 survey. In order to quantitatively analyze the relationship between $p\text{CO}_2$ drawdown and DO enhancement in spring and summer, we convert the DO enhancement into DIC change based on the classic Redfield Stoichiometry. We then use a homogenous buffer factor of the carbonate system (i.e., Revelle factor) to transfer the DIC change (induced by the DO enhancement) into $p\text{CO}_2$ change at a given temperature. The Revelle factor is defined as the ratio of fractional change in seawater $p\text{CO}_2$ to the fractional change in total DIC after re-equilibration, i.e., $\{[\partial p\text{CO}_2/p\text{CO}_2]/[\partial \text{DIC}/\text{DIC}]\}$ at a given temperature, salinity and alkalinity (Sundquist et al., 1979). In the northern ECS, the recent Revelle factor in the surface water is estimated to be 9 – 10.5 (Zhai et al., unpublished data). Note that the air-equilibrated surface DIC ranged 1850 – 2080 $\mu\text{mol kg}^{-1}$ (Zhai et al., 2007). This value was adopted in our Revelle factor related deduction.

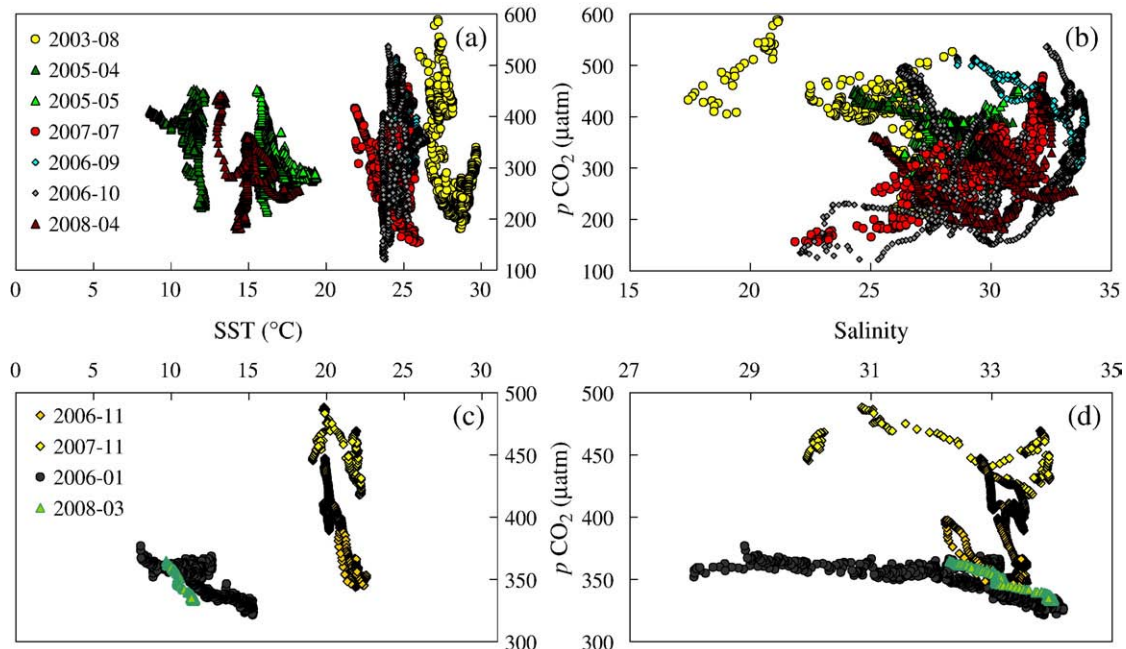


Fig. 5. Relationships among $p\text{CO}_2$, temperature and salinity in the outer Changjiang Estuary in April – October (panels a and b) and in November – March of the following year (panels c and d). Note the different salinity scale between panels (b) and (d).

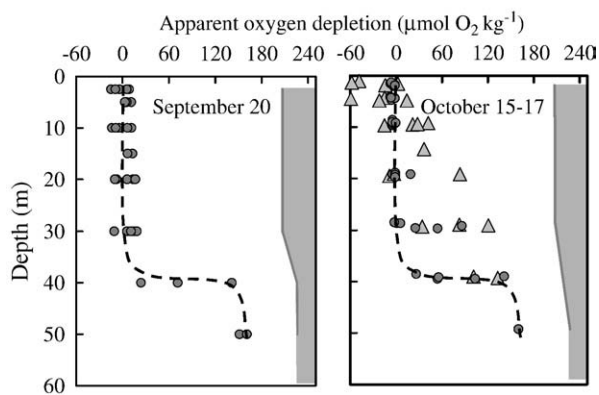


Fig. 7. Apparent oxygen depletion in the water column of the outer Changjiang Estuary in September – October, 2006. Sampling stations refer to panels (f) and (g) of Fig. 2. The upward facing triangles show coastal data (west to 123°E), while the shadowed circles mean nearshore data (123° – 124°30'E). Broken lines in the two panels show the same vertical profile of oxygen depletion. The shadowed areas mean zero oxygen. The saturated DO concentration is calculated from the Benson and Krause (1984) equation and local air pressure.

concentration in May compared with the peak values in April (Fig. 3c) supported such a pattern.

Autumn was the only season when the outer Changjiang Estuary tended to emit CO₂ (Fig. 4c). Associated with the CO₂ degassing was a slight DO deficit as compared with the air equilibrium level (Table 2; Fig. 4d), especially in early November 2007 (DO saturation ~92 ± 7%). Such a seasonal signal in autumn as a source of atmospheric CO₂ may be associated to complex physical and biogeochemical processes, such

as the low biological productivity in autumn (Gong et al., 2003). Alternatively, that the study area became a source to the atmospheric CO₂ may also be associated with the collapse of summer stratification and thereby a recovery of bottom hypoxia in autumn.

Further to the argument by Shim et al. (2007) that the northern ECS may serve as a seasonally weak source for the atmospheric CO₂ in autumn due to the seasonally enhanced vertical mixing, we contend that the bottom hypoxia was weakened by vertical mixing in October (Fig. 7) and eventually disappeared in November. As a consequence, the hypoxic and CO₂-rich bottom water became mixed and degassed CO₂ to the atmosphere in late autumn as shown in Fig. 4c.

To justify this hypothesis, we conducted a first order estimation for the possible pCO₂ level shortly after the bottom hypoxia disintegration. If the bottom oxygen depletion was represented by the measured values of 150 – 160 μmol O₂ kg⁻¹ (Fig. 7), which is consistent with the typical hypoxic DO of ~60 μmol O₂ kg⁻¹ (Li et al., 2002) and the saturated oxygen concentration is ~225 μmol O₂ kg⁻¹ (Fig. 7), the bottom excess dissolved inorganic carbon (DIC) could be estimated as ~120 μmol kg⁻¹, based on the classic Redfield stoichiometry. If the bottom 20 m (Li et al., 2002) low-oxygen – high-CO₂ water mixed with the well-ventilated upper water of ~40 m (Fig. 7), the average water column excess DIC could be ~40 μmol kg⁻¹. Using a typical Revelle factor (RF) of ~10 (Zhai et al., unpub.) and the air-equilibrated surface DIC as ~2000 μmol kg⁻¹ (Zhai et al., 2007) and the air-equilibrated surface pCO₂ as ~380 μatm (Fig. 4c), we can estimate the excess pCO₂ via $\Delta pCO_2 = \Delta DIC / DIC_{avg} \times RF \times pCO_{2,avg} = 40 / 2000 \times 10 \times 380 = 76 \mu\text{atm}$. Therefore the aquatic pCO₂ should go up to 380 + 76 = 456 μatm when the bottom hypoxia collapsed. This predicted value is at the upper limit of our measured values in late November

Table 3
Summary of sea – air CO₂ flux calculations in the outer Changjiang Estuary under study.

Surveying dates	Mean ΔpCO_2 μatm	Wind speed ^a m s ⁻¹	Estimated fluxes ^b (mmol CO ₂ m ⁻² day ⁻¹)	
			Surveying average	Seasonal average
January 01 – 03, 2006	-37 ± 17	10.5 ± 1.2 (6.5 – 13.9)	-10.4 (-12.8 to -8.2)	-10.4 ± 2.3 (winter)
April 06 – 09, 2005	-10 ± 40	5.6 ± 1.0 (2.2 – 8.0)	-0.82 (-1.14 to -0.56)	-8.8 ± 5.8 (spring)
May 13 – 16, 2005	-67 ± 47	9.3 ± 1.7 (6.4 – 14.2)	-14.8 (-20.8 to -9.9)	
March 30, 2008	-38 ± 12	13.2 ± 1.2 (10.3 – 17.4)	-16.8 (-19.9 to -14.0)	
April 01 – 08, 2008	-68 ± 14	5.5 ± 3.1 (0.1 – 14.7)	-5.3 (-12.9 to -1.0)	
April 08 – 10, 2008	-75 ± 25	10.4 ± 4.9 (1.3 – 23.1)	-20.7 (-44.9 to -5.8)	
April 11 – 18, 2008	-72 ± 12	5.9 ± 2.0 (0.8 – 11.8)	-6.4 (-11.4 to -2.8)	
April 18 – 19, 2008	-89 ± 37	2.4 ± 0.7 (0.9 – 4.9)	-1.3 (-2.3 to -0.6)	
April 28 – 29, 2008	-89 ± 68	N/A	-8.4 ^c (-17.5 to -2.6)	
August 25–27, 2003	-45 ± 110	4.7 ± 1.1 (3.3 – 8.5)	-2.5 (-3.9 to -1.5)	-4.9 ± 4.0 (summer)
July 01 – 06, 2007	-74 ± 72	6.3 ± 3.6 (0.8 – 14.5)	-7.2 (-17.9 to -1.3)	
September 20, 2006	22 ± 57	5.1 ± 0.5 (4.2 – 6.2)	1.4 (1.1 to 1.7)	2.9 ± 2.5 (autumn)
October 15, 2006	-45 ± 82	N/A	-4.2 ^c (-5.6 to -3.0)	
November 20 – 24, 2006	4 ± 32	7.2 ± 1.4 (4.4 – 10.4)	0.50 (0.33 to 0.70)	
November 01 – 10, 2007	64 ± 22	6.4 ± 2.0 (2.1 – 11.5)	6.6 (3.1 to 11.3)	

^a Mean wind speed along the cruise tracks, recorded from an onboard weather station at 10-m height and expressed as mean ± S.D. The data ranges are also presented.

^b CO₂ sea – air fluxes based on the mean ΔpCO_2 , mean wind speed and Wanninkhof (1992) air – sea transfer velocity. A positive value represents the net CO₂ exchange from sea to the atmosphere and a negative value refers to the net CO₂ exchange from the atmosphere to the sea. Data ranges are based on the S.D. of the wind speed.

^c In order to estimate air – sea CO₂ fluxes in the absence of field measured wind speed (i.e. the 28 – 29 April 2008 and 15 October 2006 surveys), we extrapolated the wind speed from the monthly average (April 2008) and neighboring months (September and November 2006) respectively.

2006 (343 – 448 μatm) and consistent with the values measured in early November 2007 ($450 \pm 21 \mu\text{atm}$) (Table 2).

Another piece of evidence pointing to the mixing-enhanced CO_2 degassing is derived from our summer data set. We noticed a significant CO_2 emission in the southern part of the July 2007 cruise track (Figs. 2e, 3a), which was associated with a DO drawdown of $\sim 20\%$ (DO saturation from $\sim 120\%$ down to $95\% - 100\%$). Most significantly, ~ 20 h of strong southwest wind ($10 - 16 \text{ m s}^{-1}$ vs. $1 - 5 \text{ m s}^{-1}$ before the event) was observed at the same time. Such a strong wind event may certainly have overthrown the stratified water column and resulted in a significant CO_2 degassing event in summer from the low-oxygen (and thereby high- $p\text{CO}_2$) bottom water. It should be pointed out that the fundamental relationship between hypoxia and CO_2 air – sea exchange needs further investigation.

4.2. Air – sea CO_2 flux estimation

Table 3 summarizes sea – air CO_2 flux calculations along the cruise tracks. If we assume that these cruise track fluxes are representative to the outer Changjiang Estuary region under study, we obtained an overview of the seasonal variation of CO_2 air–sea exchange in the outer Changjiang Estuary (Fig. 8). In this study, we use the Wanninkhof (1992) equation so that our results would be comparable with those of most other studies.

In winter, the influx was the largest, reaching $-10.4 \pm 2.3 \text{ mmol CO}_2 \text{ m}^{-2} \text{ day}^{-1}$ (Table 3). This high CO_2 influx was primarily driven by the high wind speed in winter while air – sea $p\text{CO}_2$ differences in this season were actually smaller than those in spring and summer (Table 3). Our estimate for winter is in agreement with the flux value estimated by Wang et al. (2000), i.e. between -6.5 and $-11.0 \text{ mmol CO}_2 \text{ m}^{-2} \text{ day}^{-1}$ based on the $p\text{CO}_2$ data from Tsunogai et al. (1997).

In spring, the greatest uncertainty in the air – sea CO_2 flux estimation was the wind speed. In April 2008 for example, because average wind speed varied between 2.4 m s^{-1} and 10.4 m s^{-1} during different surveying legs (Table 3), a large range of air–sea CO_2 flux was estimated (between -1.3 and $-20.7 \text{ mmol m}^{-2} \text{ day}^{-1}$) based on similar air – sea $p\text{CO}_2$ differences (Table 3). Despite such uncertainties, spring was one of the major CO_2 uptake seasons of the year, with a significant CO_2 influx of $-8.8 \pm 5.8 \text{ mmol m}^{-2} \text{ day}^{-1}$.

In summer, both surveys indicated that the outer Changjiang Estuary served as a sink of atmospheric CO_2 with an air – sea CO_2 flux of $-4.9 \pm 4.0 \text{ mmol m}^{-2} \text{ day}^{-1}$ (Table 3). This is consistent with the local intensive primary production in summer (Gong et al., 2003).

In autumn, we observed very complicated intra-seasonal variations of air – sea CO_2 flux in 2006 as pointed out above. Nevertheless, our estimate of CO_2 emission flux in autumn was $2.9 \pm 2.5 \text{ mmol m}^{-2}$

day^{-1} (Table 3). Tsunogai et al. (1997) report that the west part of the ECS absorbed CO_2 from the atmosphere during their autumn cruise (October 1993). However in this study, the outer Changjiang Estuary and an even larger area of the ECS may have equilibrated with the atmospheric CO_2 or even emitted CO_2 to the atmosphere during most of the autumn (Fig. 4c). Shim et al. (2007) also suggest that the northern ECS which they studied acts as a weak source for atmospheric CO_2 in autumn.

It must be pointed out that $p\text{CO}_2$ variability in our study area was still significant both in time and space. It is also noted that the largest uncertainty in the air – sea CO_2 flux estimation was actually from wind speed variability and the gas transfer velocity. Nevertheless, the outer Changjiang Estuary served as a moderate or significant sink of atmospheric CO_2 in winter, spring and summer, while it became a net source in autumn (Fig. 8). Based on the Wanninkhof (1992) air – sea CO_2 gas transfer velocity equation of wind speed, the annually integrated sea – air CO_2 flux in the outer Changjiang Estuary was estimated as $-1.9 \pm 1.3 \text{ mol m}^{-2} \text{ yr}^{-1}$ (Fig. 8; Table 3). As a comparison, if we use the gas transfer velocity function of Sweeney et al. (2007), this estimated flux would be lower, by $\sim 12\%$.

5. Conclusion

This study showed that, the outer Changjiang Estuary as a whole served as a net sink of atmospheric CO_2 on a yearly basis. It is known that the Changjiang River delivers substantial CO_2 -rich fresh water into the ECS in spring and summer, and the excess CO_2 must have been consumed, therefore, by biological productivity. In autumn, most products of the primary production were recycled in the water column and CO_2 degassing may even have preponderated over the biological fixation process. However, the outer Changjiang Estuary is, in general, a net autotrophic regime during warm seasons.

In the context of the entire ECS, the sea – air CO_2 flux in the outer Changjiang Estuary was double the recent sea – air CO_2 flux estimation for the northern ECS ($-0.87 \text{ mol m}^{-2} \text{ year}^{-1}$, Shim et al., 2007). This study, therefore, has demonstrated once more that air – sea CO_2 exchange substantially varies in different regimes of the ECS. A province-based approach in terms of physical and biogeochemical features would be in order if one is to reliably consider the regional air – sea CO_2 fluxes as being representative of the global continental shelf (Cai et al., 2006). The outer Changjiang Estuary is clearly one of these important regimes.

Acknowledgements

This research was supported by the Natural Science Foundation of China through grants #40876040, #40821063 and #40490264 (China-SOLAS). Sampling cruises were partially supported by the China Sea Open Cruise 2006 using R/V Kexue 3 (Institute of Oceanology, CAS, China), the National High-Tech Research and Development Program (“863” Program) of China (via the project of Quality Control / in situ Standardization Experiment 2007) and the National Basic Research Program (“973” Program) of China (grant #2005CB422300). The manuscript preparation was supported by Key Laboratory of Marine Ecosystem and Biogeochemistry, SOA, China through contract # LMEB200802 and by State Key Laboratory of Satellite Ocean Environment Dynamics (the second Institute of Oceanology, SOA, China) through Open Funds (contract # SOED0906). We thank Baoshan Chen, Jinwen Liu, Gui Chen, Zhimian Cao and Yi Wang for assistance in the data collection. The crews of R/Vs Dongfanghong II and Kexue 3 provided much help during the sampling cruises. We thank Drs Lingxi Zhou and Lixin Liu and Mr Min Wen for their help during the CO_2 reference gas calibration experiments and Professor John Hodgkiss for his assistance with English. Finally, we are grateful to two anonymous reviewers for their constructive comments and suggestion on the manuscript.

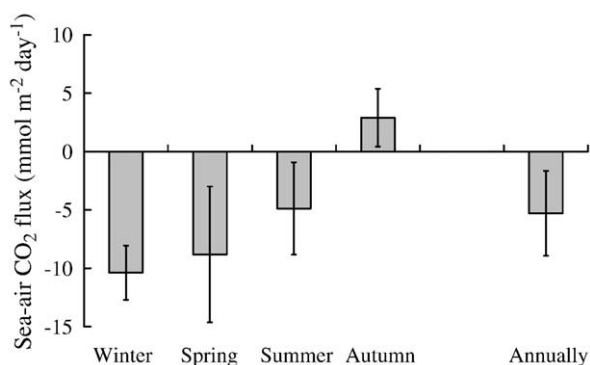


Fig. 8. Seasonal sea – air CO_2 fluxes in the outer Changjiang Estuary. The study area is shown in Figs. 1 and 2. The errors are estimated as accumulative uncertainty (S.D.) from wind speed variability and variations between different surveys in the same season of the year.

References

- Benson, B.B., Krause, D., 1984. The concentration and isotopic fractionation of oxygen dissolved in fresh water and seawater in equilibrium with the atmosphere. *Limnol. Oceanogr.* 29, 620–632.
- Borges, A.V., Delille, B., Frankignoulle, M., 2005. Budgeting sinks and sources of CO₂ in the coastal ocean: diversity of ecosystems counts. *Geophys. Res. Lett.* 32, L14601. doi:10.1029/2005GL023053.
- Cai, W.-J., Dai, M.H., 2004. Comment on "Enhanced open ocean storage of CO₂ from shelf sea pumping". *Science* 306, 1477.
- Cai, W.-J., Dai, M.H., Wang, Y.C., 2006. Air – sea exchange of carbon dioxide in ocean margins: a province-based synthesis. *Geophys. Res. Lett.* 33, L12603. doi:10.1029/2006GL026219.
- Chen, C.-T.A., Borges, A.V., 2009. Reconciling opposing views on carbon cycling in the coastal ocean: continental shelves as sinks and nearshore ecosystems as sources of atmospheric CO₂. *Deep Sea Res., Part 2* 56, 578–590.
- Chen, C.-C., Gong, G.-C., Shiah, F.-K., 2007. Hypoxia in the East China Sea: one of the largest coastal low-oxygen areas in the world. *Mar. Environ. Res.* 64, 399–408.
- Chen, C.-T.A., Zhai, W.D., Dai, M.H., 2008. Riverine input and air – sea CO₂ exchanges near the Changjiang (Yangtze River) Estuary: status quo and implication on possible future changes in metabolic status. *Cont. Shelf Res.* 28, 1476–1482.
- Chen, C.S., Zhu, J.R., Beardsley, R.C., Franks, P.J.S., 2003. Physical–biological sources for dense algal blooms near the Changjiang River. *Geophys. Res. Lett.* 30, 1515. doi:10.1029/2002GL016391.
- Gong, G.-C., Chen, Y.-L.L., Liu, K.-K., 1996. Chemical hydrography and chlorophyll *a* distribution in the East China Sea in summer: implications in nutrient dynamics. *Cont. Shelf Res.* 16, 1561–1590.
- Gong, G.-C., Wen, Y.-H., Wang, B.-W., Liu, G.-J., 2003. Seasonal variation of chlorophyll *a* concentration, primary production and environmental conditions in the subtropical East China Sea. *Deep-Sea Res., Part 2* 50, 1219–1236.
- Hu, D.X., Yang, Z.S., 2001. Key processes of marine fluxes in the East China Sea. China Ocean Press, Beijing, China. 204pp. (in Chinese).
- Li, D.J., Zhang, J., Huang, D.J., Wu, Y., Liang, J., 2002. Oxygen depletion off the Changjiang (Yangtze River) Estuary. *Sci. China, Ser. D Earth Sci.* 45, 1137–1146.
- Muller-Karger, F.E., Varela, R., Thunell, R., Luerssen, R., Hu, C., Walsh, J.J., 2005. The importance of continental margins in the global carbon cycle. *Geophys. Res. Lett.* 32, L01602. doi:10.1029/2004GL021346.
- Shim, J., Kim, D., Kang, Y.C., Lee, J.H., Jang, S.-T., Kim, C.-H., 2007. Seasonal variations in pCO₂ and its controlling factors in surface seawater of the northern East China Sea. *Cont. Shelf Res.* 27, 2623–2636.
- Sundquist, E.T., Plummer, L.N., Wigley, T.M.L., 1979. Carbon dioxide in the ocean surface: the homogenous buffer factor. *Science* 204, 1203–1205.
- Sweeney, C., Gloor, E., Jacobson, A.R., Key, R.M., McKinley, G., Sarmiento, J.L., Wanninkhof, R., 2007. Constraining global air – sea gas exchange for CO₂ with recent bomb ¹⁴C measurements. *Global Biogeochem. Cycles* 21, GB2015. doi:10.1029/2006GB002784.
- Tan, Y., Zhang, L.J., Wang, F., Hu, D.X., 2004. Summer surface water pCO₂ and CO₂ flux at air – sea interface in western part of the East China Sea. *Oceanol. Limnol. Sin.* 35, 239–245 (in Chinese).
- Tsunogai, S., Watanabe, S., Nakamura, J., Ono, T., Sato, T., 1997. A preliminary study of carbon system in the East China Sea. *J. Oceanogr.* 53, 9–17.
- Tsunogai, S., Watanabe, S., Sato, T., 1999. Is there a "continental shelf pump" for the absorption of atmospheric CO₂? *Tellus* 51B, 701–712.
- Wang, S.L., Chen, C.T.A., Hong, G.H., Chung, C.S., 2000. Carbon dioxide and related parameters in the East China Sea. *Cont. Shelf Res.* 20, 525–544.
- Wanninkhof, R., 1992. Relationship between wind speed and gas exchange over the ocean. *J. Geophys. Res.* 97, 7373–7382.
- Wei, H., He, Y.C., Li, Q.J., Liu, Z.Y., Wang, H.T., 2007. Summer hypoxia adjacent to the Changjiang Estuary. *J. Mar. Syst.* 67, 292–303.
- Weiss, R.F., 1974. Carbon dioxide in water and seawater: the solubility of a non-ideal gas. *Mar. Chem.* 2, 203–215.
- Wong, G.T.F., Chao, S.-Y., Li, Y.-H., Shiah, F.-K., 2000. The Kuroshio edge exchange processes (KEEP) study – an introduction to hypotheses and highlights. *Cont. Shelf Res.* 20, 335–347.
- Zhai, W.D., Dai, M.H., Cai, W.-J., Wang, Y.C., Wang, Z.H., 2005. High partial pressure of CO₂ and its maintaining mechanism in a subtropical estuary: the Pearl River estuary, China. *Mar. Chem.* 93, 21–32.
- Zhai, W.D., Dai, M.H., Guo, X.H., 2007. Carbonate system and CO₂ degassing fluxes in the inner estuary of Changjiang (Yangtze) River, China. *Mar. Chem.* 107, 342–356.
- Zhang, Y.H., Huang, Z.Q., Ma, L.M., Qiao, R., Zhang, B., 1997. Carbon dioxide in surface water and its flux in East China Sea. *J. Oceanogr. Taiwan Strait* 16 (1), 37–42 (in Chinese).
- Zhang, L.J., Wang, B.Y., Zhang, J., 1999. pCO₂ in the surface water of the East China Sea in winter and summer. *J. Ocean U. Qingdao (Suppl.)* 149–153 (in Chinese).
- Zhang, Y.Y., Zhang, J., Wu, Y., Zhu, Z.Y., 2007. Characteristics of dissolved oxygen and its affecting factors in the Yangtze Estuary. *Environ. Sci.* 28, 1649–1654 (in Chinese).